

Pressure data for various flow channels in proton exchange membrane (PEM) fuel cell

Son-Ah Cho, Pil-Hyong Lee, Sang-Seok Han and Sang-Soon Hwang*

Dept. of Mechanical engineering, University of Incheon, Incheon 402-749 Korea

(Manuscript Received March 2, 2007; Revised November 14, 2007; Accepted November 15, 2007)

Abstract

Micro flow channels in flow plates of fuel cells have become much narrower and longer to improve reactant flow distribution leading to increase of pumping power. Therefore it is very important to minimize the pressure drops in the flow channel because increased pumping power reduces overall efficiency. We investigated pressure drops in a micro flow channel at the anode and cathode compared to pressure losses for cold flow in straight, bended and serpentine channels. The results show that friction factors for cold flow channels could be used for parallel and bended flow channel designs for fuel cells. Pressure drop in the serpentine flow channel is the lowest among all flow channels due to bypass flow across the gas diffusion layer under reactive flow condition, although its pressure drop is highest for a cold flow condition. So the effect of bypass flow for serpentine flow channels should be considered when designing flow channels

Keywords: Friction factor; PEMFC; Electrochemical reaction; Bypass flow; Serpentine flow

1. Introduction

Flow plates in electrochemical power sources such as fuel cells contain many micro flow channels to distribute the reactant gas flow over the catalytic reactive surface. The shape, size and pattern of flow channels can significantly affect the power source's performance. Micro flow channels in flow plates have become much narrower and longer to better distribute the reactant gas flow, increasing pumping power. Therefore it is very important to minimize pressure drops in the gas flow because increased pumping power reduces the overall efficiency. Typically the mass flow and channel size are small, and the flow is expected to be laminar, so pressure losses depend strongly on the Reynolds Number. The aspect and curvature ratios are known to be critical factors to determine the pressure drops in bended flow chan-

nels. Many researches about pressure losses in non-reacting flow in fine flow channels are available in the literature. Measurements of the velocity field in bends of circular and square cross sections of various diameter radius ducts have been carried out [1]. Miyaka et al [2] reported numerical simulation on curved ducts with a rectangular cross-section and described the inlet and outlet flow field, and Ward-Smith [3] summarized very well experimental data of the friction factor for pipes with various curvature ratios. Maharudrayya [4] investigated the effect of the geometric parameters and the Reynolds Number on the flow pattern and the pressure loss characteristics, so some correlations between the above factors and pressure losses have been derived non-numerically for the effects on pressure drop of aspect ratio, Reynolds Number and permeability of gas diffusion media.

Lan [5] studied the pressure drop considering channel-to-channel crossover flow in a serpentine flow channel, but it is questionable whether the above

*Corresponding author. Tel.: +82 32 770 8417, Fax.: +82 32 770 8410
E-mail address: hwang@incheon.ac.kr
DOI 10.1007/s12206-007-1108-4

friction factor data for cold flow could be used to design a flow channel for fuel cells because hydrogen consumption at the anode and oxygen consumption and water generation at the cathode can change the flow field in the flow channel greatly. It is therefore necessary to include the effects of electrochemical reaction on flow fields in anode and cathode flow channels.

As in recent studies about flow channels with electro-chemical reactions, Yuan [6] and Rawool [7] investigated numerical simulation on the gas flow and heat transfer in parallel and curved flow channels of PEMFC, but limited data for friction loss were reported. For this paper we investigated the pressure drops in micro flow channels of various geometries at the anode and cathode with electro-chemical reactions, and compared them to pressure losses in corresponding non-reacting flow channels. Modified Fluent code was used for computational analysis. Through numerical simulation, friction coefficients for flow channels of various geometries were analyzed as a function of the Reynolds Number, and detailed contours of current density and velocity vector were plotted to understand the pressure variations along the channel.

Table 1. Dimension of fuel cell.

Description	Value
Cell/electrode length (cm)	10
Gas channel height (cm)	0.12
Gas channel width (cm)	0.08
Anode GDL thickness (cm)	0.0375
Membrane thickness (cm)	0.01
catalyst layer thickness (cm)	0.0025
Cathode GDL thickness (cm)	0.0375

Table 2. Initial conditions.

Description	Value
Relative humidity of inlet fuel stream (%)	100
Anode stoichiometry	1
Cathode stoichiometry	1
Cell voltage (V)	0.7
Inlet nitrogen-oxygen mole fraction ratio	0.79/0.21
Cell temperature (K)	353
Electrode porosity (ϵ)	0.7
Anode/cathode output pressure (atm)	1.0

2. Computational methods

Modified Fluent code was used for numerical simulation of the flow channel. It is assumed that the fluid flow is a mixture of ideal gases and incompressible laminar flow. Electrodes and catalyst layers and membranes are assumed to consist of isotropic porous material. The dimension and initial conditions for fuel cell simulation are given in Tables 1 and 2.

2.1 Governing equations

Mass Conservation of Mixture

$$\nabla \cdot (\epsilon \rho \vec{u}) = S_m \tag{1}$$

Momentum conservation equation is based on Darcy's law (10)

$$\nabla \cdot (\epsilon \rho \vec{u} \vec{u}) = -\epsilon \nabla p + \nabla \cdot (\epsilon \mu \nabla \vec{u}) + S_u \tag{2}$$

Species conservation equation

$$\nabla \cdot (\epsilon \vec{u} C_k) = \nabla \cdot (D_k^{eff} \nabla C_k) + S_k \tag{3}$$

And, source terms are summarized in Table 3.

Current density is described by

$$I(x, y, z) = \frac{\sigma_m(x, y, z)}{t_m} \{V_{oc} - V_{cell} - \eta(x, y, z)\} \tag{4}$$

Table 3. Source terms related to the electrochemical reaction.

Source terms	Equations
S_m	$S_{H_2} + S_{H_2O_a}$ → anode side
	$S_{O_2} + S_{H_2O_c}$ → cathode side
S_u	$-\frac{\mu \vec{u}}{\beta}$
S_k	$S_{H_2} = -\frac{I(x, y, z)}{2F} M_{H_2} A_{cv}$ → anode side
	$S_{H_2O_a} = -\frac{\alpha(x, y, z)}{F} I(x, y, z) M_{H_2O} A_{cv}$ → anode side
	$S_{O_2} = -\frac{I(x, y, z)}{4F} M_{O_2} A_{cv}$ → cathode side
	$S_{H_2O_c} = \frac{1+2\alpha(x, y, z)}{2F} I(x, y, z) M_{H_2O} A_{cv}$ → cathode side

Friction factor fRe is expressed as

$$fRe = \frac{2 * D_h^2}{\mu} * \frac{\Delta P}{V * dx} \tag{5}$$

where, μ is viscosity coefficient, V is velocity and ΔP , dx are pressure drop, mesh size respectively.

Equations related to water transport is described as

$$J_{H_2O} = 2 * n_d * \frac{I(x,y,z)}{2F} : \text{Electro-osmotic drag flux} \tag{6}$$

$$J_{H_2O,backdiffusion} = -\frac{\rho_{m,dry} * D_w}{M_{m,dry}} * \frac{d\lambda}{dz} : \text{Back diffusion flux} \tag{7}$$

2.2 Boundary condition

A zero velocity condition is applied at channel wall boundary and mass flow rate for the gas-flow channel inlets is given. Ambient pressure is specified at the outlets of channel.

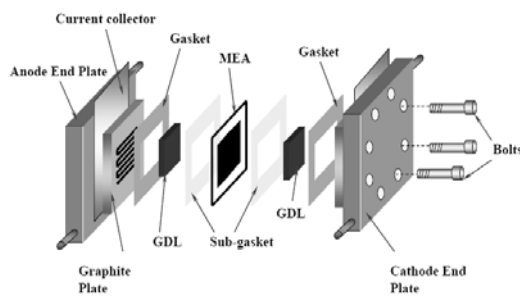
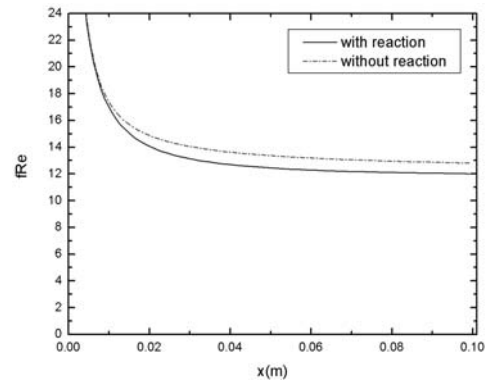


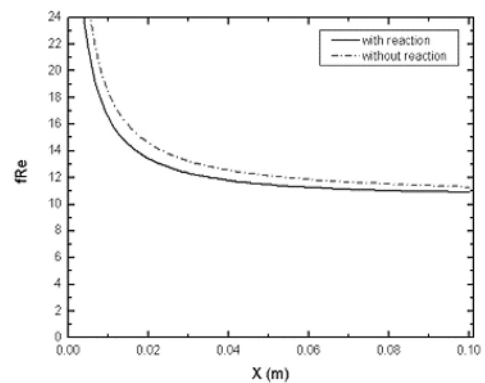
Fig. 1. Schematic of PEM fuel cell showing the location of the components.

3. Results and discussions

Fig. 1 shows a typical schematic of a proton exchange membrane (PEM) fuel cell. The cell consists of an end plate, a flow channel plate, a gas diffusion



(a)



(b)

Fig. 3. Variation of fRe along the x axis with and without reaction at anode(a) and cathode(b) side for straight channel.

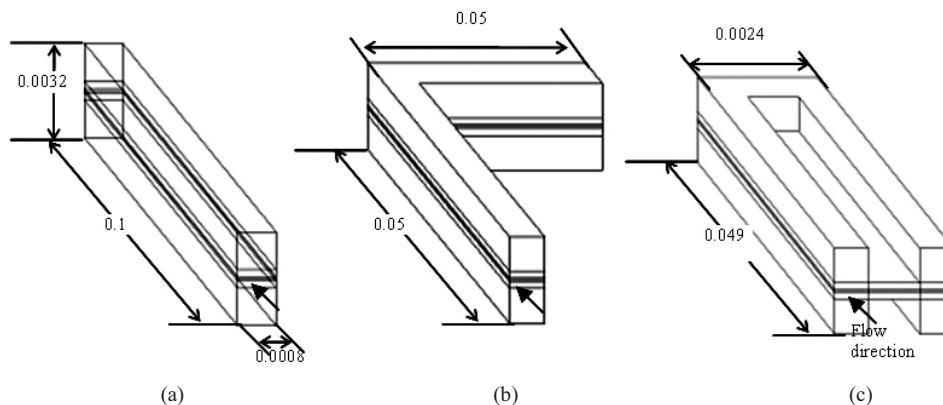


Fig. 2. Three Different types of flow channels used for numerical simulation (a) parallel type (b) bended type(c) serpentine type.

layer (GDL) and a membrane electrode assembly (MEA). The flow channel and GDL are very important for determining the optimal performance of the catalyst and the electrode. While the flow channel is used to supply hydrogen and oxidant gas to the GDL, the GDL is porous to distribute gases to unexposed areas of the flow channel, and this distribution allows for complete utilization of the catalyst area. It is very important to examine the interaction between the gas flow channel and the porous GDL to predict the pressure drop for various configurations of flow channels.

This study numerically simulated flow fields in the three different types of flow channels shown in Fig. 2 under flow conditions with and without electrochemical reactions.

Fig. 3 shows the effects of a chemical reaction on the friction factor (f_{Re}) along the channel axis for a straight channel.

A slightly lower f_{Re} value than in the figure was noticed during the chemical reaction at the anode and cathode. It is thought that hydrogen consumption at the anode, and oxygen consumption and water generation at the cathode, contribute to the decrease in density leading to the reduction in the friction factor when an electrochemical reaction occurs. This result shows a trend very similar to Yuan's work [8], which dealt with mass transfer effects on f_{Re} using numerical calculation. Variation in the friction factor along the flow axis for a bended flow channel is presented in Fig. 4, which shows a spike at the bended region of the flow channel with and without reaction. The friction factor for the two cases shows almost the same value and pattern. In order to see how the spike is generated, velocity vectors were plotted in Fig. 5. A strong recirculation zone can be seen around the cor-

ner. This zone contributes to higher friction, leading to a high pressure drop around the channel's bend.

The above results for parallel and bended flow channels show that the friction factor for a cold flow channel could reasonably be used to design a flow channel for a fuel cell. Next we investigated the friction factor for a serpentine flow channel, which has been widely used as flow channel for PEMFCs.

Fig. 6 represents the friction factor along the flow axis for a serpentine flow channel. It shows two spikes around the two bend regions, which are ex-

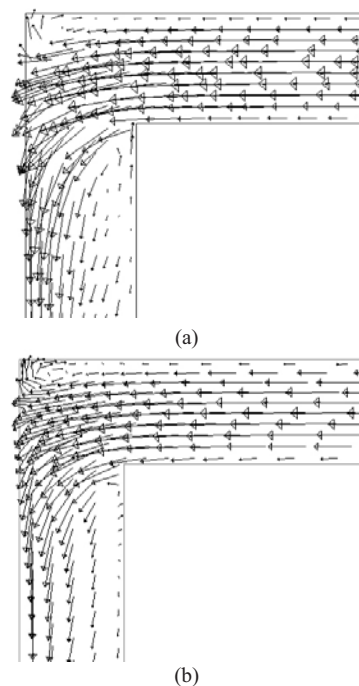


Fig. 5. Velocity vectors in bended flow channel without (a) and with (b) reaction.

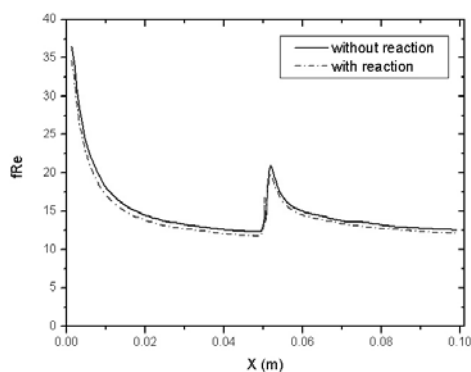


Fig. 4. Variation of friction factor along the axis with and without reaction for bended flow channel.

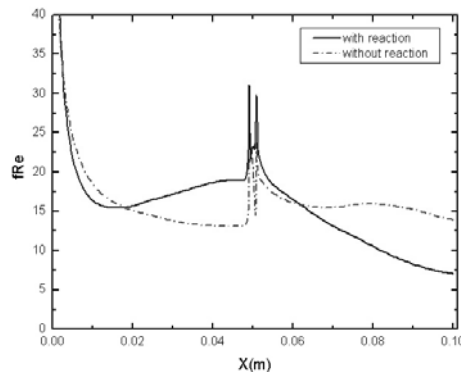


Fig. 6. Friction factors for serpentine flow channel with/without reacting condition.

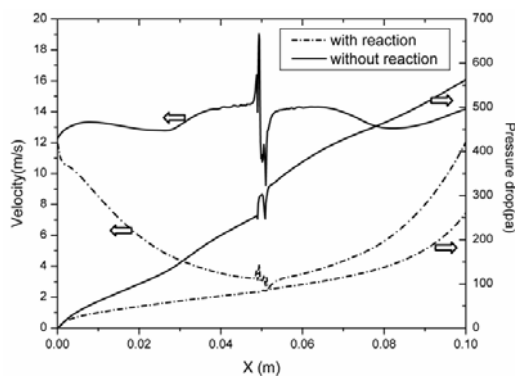


Fig. 7. pressure drop and velocity along the flow channel for serpentine flow channel with/without reaction.

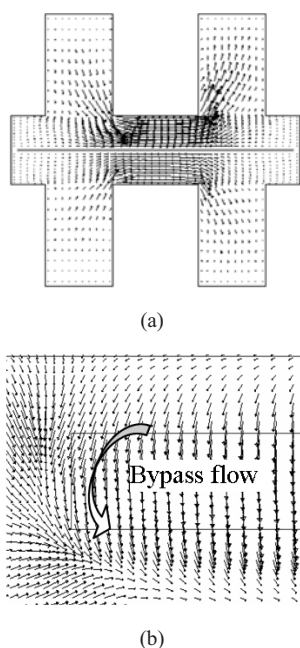


Fig. 8. Velocity vectors at the cross section (a) and top view of gas diffusion layer (b) for serpentine flow with reaction.

pected for a serpentine flow structure having two recirculation zones at the bended regions. From the figure the friction factor with reaction is higher than it without reaction before bended region following lower friction factor after bended part. So it is difficult to compare friction coefficients of two cases.

Fig. 7 is presented in order to know the pressure drop itself and velocity variation along the serpentine channel. Flow velocity with reaction before bended part is decreased sharply and then increased after bended part. The low velocity before bended part

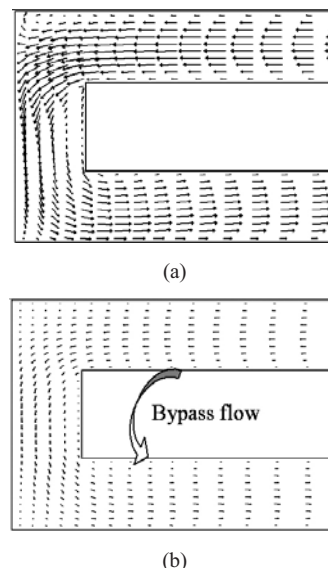


Fig. 9. Velocity vectors in flow channel for non-reacting (a) and reacting condition (b).

which is denominator of friction factor makes the friction factor higher. Figure shows that the pressure drop for serpentine flow channel with reaction is very low compared to it without reaction due to leakage of reactants by bypass flow. To find out the bypass flow, velocity vector in the gas diffusion layer during the reaction is presented in Fig. 8.

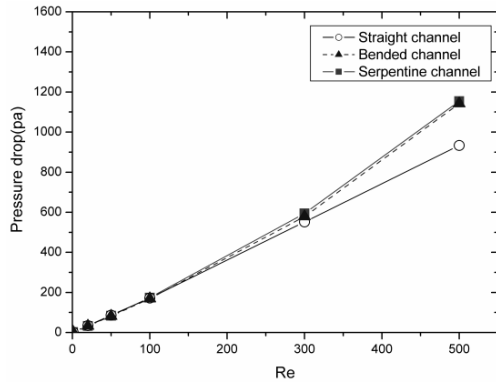
Fig. 8 (a) represents the velocity vectors at the cross section, and 8 (b) shows the velocity vectors at the top view of the gas diffusion. The figure reveals that the reactant bypasses through the gas diffusion layer to an adjacent channel, compared to a reactant with no reaction flowing only along the flow channel. This suggests that the bypass flow reduces the flow rate in the channel, which reduces friction loss.

To show the bypass flow's effect across the gas diffusion layer on the main flow within the flow channel, velocity vectors within the flow channel are presented in Fig. 9, which shows velocity vectors with non-reacting (a) and reacting flows. It shows that the flow velocity along the channel with reacting flow is much less than with non-reacting flow due to leakage from the bypass flow.

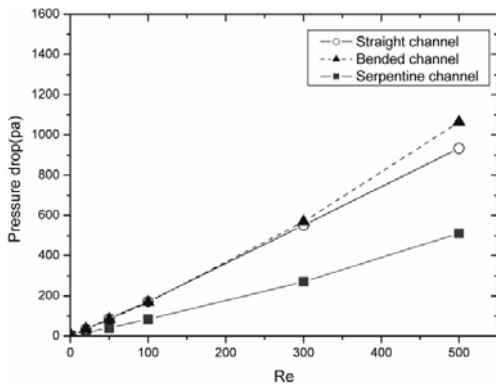
Fig. 10 shows the current density distribution in a serpentine flow channel. It is found that current density has higher value around entrance where reactants is supplied in and its concentration is high because current density is proportional to electrochemical reaction rate. And current density is also found to be



Fig. 10. Current density at the membrane.



(a)



(b)

Fig. 11. Comparison of pressure drops for Re for three flow channels without (a) and with (b) reacting condition.

high at rib region where leakage flow is strong so more reactants is supplied through the gas diffusion layer between adjacent channels.

Fig. 11 shows that the pressure drop in a serpentine flow channel is the lowest among the three flow channels under reaction condition, although its pressure drop is highest for a cold flow condition.

4. Conclusion

1. The friction factor under a chemical reaction condition at the anode and cathode channel is slightly less than with cold flow because hydrogen consumption at the anode, and oxygen consumption and water generation at the cathode, contribute to the decrease in density leading to a reduction in friction force compared to cold flow condition .

2. For parallel and bended flow channels, friction factors for the cold flow channel could reasonably be used to design a flow channel in a fuel cell.

3. The pressure drop in a serpentine flow channel is the lowest among the flow channels under a reacting flow condition due to bypass flow across the gas diffusion layer, although its pressure drop is highest during a cold flow condition. So the effect of bypass flow in a serpentine flow channel with a close adjacent channel should be considered when designing a flow channel.

Nomenclature

- A_{cv} : Specific surface area of the control volume (m^{-1})
- C : Concentration ($mol\ m^{-3}$)
- D_h : Hydraulic diameter (m)
- D_{ij}^{eff} : Effective diffusion coefficient ($m^2\ s^{-1}$)
- F : Faraday constant ($C\ mol^{-1}$)
- h : Enthalpy ($kJ\ kg^{-1}$)
- I : Local current density ($A\ m^{-2}$)
- L : Length of channel (m)
- $M_{m,dry}$: Equivalent weight of a dry membrane ($kg\ mol^{-1}$)
- P : Pressure (Pa)
- S : Source term
- T : Temperature (K)
- \vec{u} : Velocity vector ($m\ s^{-1}$)
- μ : Dynamic viscosity ($kg\ s\ m^{-2}$)
- α : Net water flux per proton flux
- ε : Porosity
- n_d : Electro-osmotic drag coefficient
- σ_m : Membrane conductivity ($ohm^{-1}\ m^{-1}$)
- $\rho_{m,dry}$: Density of a dry membrane ($kg\ m^{-3}$)
- ρ : Density of the mixture ($kg\ m^{-3}$)

References

[1] J. A. C. Humphrey, J. H. Whitelaw and G. Yee, Turbulent Flow in a Square Duct with Strong Curvature, *J. Fluid Mech.* 103 (1981) 443-463.

- [2] Y. Miyaka, T. Kazishima and T. Inaba, International Conference on Experimental Heat Transfer, Fluid Mechanics and Thermodynamics, (1988).
- [3] A. J. Ward-Smith, Internal Fluid Flow, Oxford university press, New York, USA (1980).
- [4] S. Maharudrayya, S. Jayanti and A. P. Deshpande, Pressure losses in laminar flow through serpentine channels in fuel cell stacks, *J. Power Sources* 138 (2004) 1-13.
- [5] L. Sun, P. H. Oosthuizen, B. Kim and McAuley, A numerical study of channel-to-channel flow crossover through the gas diffusion layer in a PEM-fuel-cell flow system using a serpentine channel with a trapezoidal cross-sectional shape, *Int. J. Thermal Sciences* 45 (2006) 1021-1026.
- [6] J. Yuan, M. Rokni and B. Sunden, A numerical investigation of gas flow and heat transfer in proton exchange membrane fuel cells, *Num. Heat Transfer (partA)* 44 (2003) 255-280.
- [7] A. S. Rawool, S. K. Mitra and J. G. Pharoah, An investigation of convective transport in micro proton-exchange membrane fuel cells, *J. Power Source* 162 (2006) 985-991.
- [8] A. S. Rawool, S. K. Mitra, A. Agrawal and S. Kandikar, Numerical simulation of flow through microchannels in bipolar plate, *ICMM* (2005) 2005-75251.
- [9] J. G. Pharoah, On the permeability of gas diffusion media used in PEM fuel cells, *J. Power sources* 144 (2005) 77-82.
- [10] R. B. Bird, W. E. Stewart and E. N. Lightfoot, Transport phenomena, Wiley, New York, UAS, (1960).